Scale-dependence in ΛCDM parameters inferred from the CMB: a possible sign of Early Dark Energy

Jun-Qian Jiang[1, *]

[1]*School of Physical Sciences, University of Chinese Academy of Sciences, Beijing 100049, China*

Abstract

The early dark energy (EDE) model is one of the promising solutions to the Hubble tension. One of the successes of the EDE model is that it can provide a similar fit to the ΛCDM model for the CMB power spectrum. In this work, I analyze the phenomenology of the EDE and ΛCDM parameters on the CMB temperature power spectrum and notice that this cannot hold on all scales. Thus, if the real cosmology is as described by the EDE model, the ΛCDM parameters will be scale-dependent when fitting the CMB power spectrum with the ΛCDM model, which can be hints for the EDE model. I examine CMB-S4-like observations through mock data analysis and find that parameter shifts are notable. As observations include smaller scales, I find lower H_0, n_s, ω_b and higher ω_m, $A_s e^{-2\tau}$, which will also constitute new tensions with other observations. They can serve as a possible signal for the EDE model.

---

* jiangjunqian21@mails.ucas.ac.cn; jiangjq2000@gmail.com

I. INTRODUCTION

The Hubble tension [1–9] is one of the greatest conflicts encountered in cosmological observations today. The Hubble constant H_0 inferred from the CMB power spectrum observation prefers a low value. For example, Planck 2018 reported $H_0 = (67.4 \pm 0.5)$ km/s/Mpc [10]. In contrast, local measurements, which are independent of the cosmological model, prefer a large value. Based on observations of Cepheid-calibrated SNeIa, the SH0ES team reported $H_0 = (73.04 \pm 1.04)$ km/s/Mpc [11]. Depending on different observations, there is a tension of about $4 \sim 6\sigma$ [1].

This tension calls for some modification of the ΛCDM model. These modifications to cosmology can usually be divided into post-recombination solutions and pre-combination solutions. The former's capacity to resolve Hubble tension is limited by measurements from BAO and uncalibrated SNeIa [12–24], which makes pre-recombination solutions more likely. One of the promising solutions is a new pre-combination component named Early Dark Energy (see e.g. Refs.[25–43]), although it also faced some challenges (see a recent review Ref. [44]). In principle, for a given early dark energy model, it can be fitted directly to the observational data and can be detected by future CMB observations if the required new physics is indeed as it is described. However, the early dark energy model is a class of models with numerous realizations that have not exactly the same phenomenologies. These phenomenological differences will change their fit to CMB observations, which will ultimately lead to the fact that it may be difficult to detect by future CMB observations if we are not lucky enough to test the correct EDE model. Actually, we have already seen in recent observations that current CMB data has different levels of preference for different EDE models [45]. Therefore, instead of fitting with a specific EDE model, a feasible approach is to observe the behavior when fitting with the ΛCDM model. At the same time, when detection capabilities are stronger, fitting with all features will inevitably introduce differences between different EDE models. Thus, to make the results more generalizable, it is necessary to compress these features into a few that are less sensitive to differences between EDE models, typically focusing on the relative relationships of the quantities rather than their specific values. Although these compressed features cannot strictly prove the correctness of the EDE model, they can serve as a hint or a way to rule out the EDE model. For example, the compressed features considered in Refs. [46, 47] are whether there is a significant difference

between the sound horizon-dependent H_0 and the sound horizon-independent H_0. Here, I consider the scale dependence of the ΛCDM parameters inferred from the CMB.

The scale inconsistency of the ΛCDM model, if it indeed exists, could advance our understanding of cosmological tensions and suggest the possibility of new physics [48]. Actually, there appears to be some inconsistency in the fit of the ΛCDM to the current CMB observations, both within the same observations and across different observations. For example, there is a $\gtrsim 2\sigma$ discrepant between some parameters inferred from low-ℓ ($\ell < 800(1000)$) and full-ℓ Planck 2015 TT power spectrum [49, 50]. Meanwhile, the CMB lensing effect acting on the Planck CMB power spectrum also appears to be stronger than predicted by the ΛCDM model [10, 49, 51, 52] (see also Refs.[53–57]). In addition, the Planck results also seem to have some discrepancies with the results of other CMB observations such as ACT [55] and SPT-3G [56, 57], see Refs.[58–62] for discussions.

In this work, I investigate the role of the general EDE model and the ΛCDM parameters for the CMB power spectrum. For simplicity, I restrict the analysis to the temperature (TT) power spectrum. [1] I find that the degeneracy between the EDE model and the ΛCDM model becomes more and more imperfect as the range of scales covered by the CMB observations increases. If our universe is as described by the EDE model, then as future CMB observations are able to cover smaller scales, a predictable result is that when the ΛCDM model is used to fit the observations, its parameters will shift, i.e., have scale dependencies.

This paper is organized as follows: In section II, I discuss the main phenomenology of EDE on the temperature power spectrum and the reasons for the corresponding shifts in cosmological parameters during data fitting. The results of the parameter shifts when fitting with the ΛCDM model are presented and discussed in section III. In section A, I demonstrate the robustness of the conclusions with respect to the details of the EDE model. In addition, section B presents the results of parameter shifts when the polarization power spectrum is included in the analysis.

---

[1] Another reason is that the polarization spectrum has a more significant dependence on the details of the EDE model implementation than the temperature spectrum, which is what I want to avoid here. For example, it seems that the Planck polarization spectrum is related to the preference of a flat potential at high redshift for the axion-like EDE [30], in contrast to the rock'n'roll model [28]. Ref.[29] found that ADE and axion-like EDE have very similar fits for the TT spectrum, but exhibit different fits for the polarization spectrum.

II. EDE PHENOMENOLOGY AND THE SHIFT OF COSMOLOGICAL PARAMETERS

Early dark energy (EDE) is a component assumed to exist prior to the recombination that behaves like dark energy, i.e., with the equation of state $w_i \sim -1$. Its energy fraction grows gradually and then decays before the recombination. The observations favor the peak of the EDE energy fraction around the matter radiation equality, allowing for a maximum reduction of r_s [26]. The CMB observations also prefer that the energy decays faster than the radiation, i.e. the equation of state during the decay period $w_f \gtrsim 1/3$ [26, 29]. There are many implementations that achieve the rapid decay of energy, such as oscillations [26, 28], a runaway potential [29], anti-de Sitter (AdS) phase [33, 63], and phase transition [31].

Below I briefly summarize the general properties of EDE, its implications for the CMB TT power spectrum, and how the other ΛCDM parameters shift. This means that I will not delve into the perturbative properties of EDE, although this is important for data fitting [25]. And there seems to be no qualitative difference in their implications for the CMB TT power spectrum between viable EDE models [42].

To aid understanding, I choose ϕ^4 AdS-EDE [33, 64, 65] as an example. I chose the best-fit points of AdS-EDE and ΛCDM for state-of-the-art CMB + BAO + SNeIa + H_0 observations. Where the CMB dataset combination includes the Planck 2018 (PR3) `Commander` likelihood [66] for the low-ℓ TT spectrum, the PR4 `lollipop` likelihood [67–69] for the low-ℓ EE spectrum, the PR4 `CamSpec` likelihood [70] for the high-ℓ TTTEEE spectrum, ACT DR4 [55] and SPT-3G Y1 [56, 57] TTTEEE spectrum. $\ell > 1800$ part of the ACT TT spectrum is removed to avoid the cross-correlation, following Ref.[55]. The BAO dataset consists of 6dF [71], SDSS [72–74], and DESI Y1 [75] datasets, following Ref.[75]'s way of combining the latter two. I also used the Pantheon+ measurement [76] on the SNeIa and the SH0ES data [11]. The values of the parameters are shown in Table I.

Here, I use five quantities to characterize the effect of different components/parameters on the CMB TT power spectrum:

- The angular separation of acoustic peaks $\theta_s^* = r_s^*/D_A$, where D_A is the angular distance to the last scattering surface and r_s^* is the sound horizon at CMB last-scattering:

$$r_s^* = \int_{z^*}^{\infty} \frac{c_s(z)}{H(z)} \mathrm{d}z \,, \tag{1}$$

Parameters	ΛCDM	EDE
$\ln(1 + z_c)$		8.07
f_{EDE}		0.11
H_0	68.33	72.22
n_s	0.9713	0.9913
$\omega_b = \Omega_b h^2$	0.0223	0.0229
$\omega_c = \Omega_c h^2$	0.1173	0.1343
$\ln(10^{10} A_s)$	3.0529	3.0847
τ	0.0592	0.0552
$\omega_m = \Omega_m h^2$	0.1403	0.1578
$10^9 A_s e^{-2\tau}$	1.8811	1.9576
$100\,\theta_s^*$	1.0446	1.0437
$100\,\theta_D$	0.3232	0.3262
$\mathrm{PH}_1/\mathrm{PH}_2$	2.197	2.193
$C_{\mathrm{peak}}^{\phi\phi}$	1.360×10^7	1.395×10^7
$C_{\mathrm{peak}}^{\mathrm{TT,\ EISW}}$	409.0	405.5

TABLE I. The best-fit values of the current observations (described in the text) for parameters of the two models.

z_* is the redshift to the CMB last-scattering surface[2] and c_s is the sound speed.

- The angular size $\theta_D = r_D/D_A$ of the diffusion damping scale r_D.

- The ratio between the first and second acoustic peak $\mathrm{PH}_1/\mathrm{PH}_2$. It is related to the shift of the zero point of the acoustic oscillation. Meanwhile, since the position of the first peak is close to the project sound horizon at the matter-radiation equality, it will also be related to the "potential envelope" [77–79]. This effect arises from the decay of the potential energy during and before the matter-radiation equality, which leads to a near-resonant driving of the modes entering the horizon. It leads to an exponential dependence of the CMB power spectrum if the diffusion damping is removed [78]:

$$1 + A\exp(-1.4\ell_{\mathrm{eq}}/\ell), \qquad (2)$$

---

[2] A better way is to use visibility-averaged sound horizon [17], same as for the r_D below.

	EDE	H_0	ω_m	n_s	ω_b	$A_s \exp(-2\tau)$
θ_s^*	-2.6%	$+1.1\% = 0.2\Delta$	$+1.6\% = 0.13\Delta$	0	$-0.2\% = -0.08\Delta$	0
θ_D	-0.9%	$+1.1\% = 0.2\Delta$	$+1.4\% = 0.12\Delta$	0	$-0.6\% = -0.3\Delta$	0
$\mathrm{PH_1/PH_2}$	$+0.7\%$	0	$-0.6\% = -0.05\Delta$	$-1.8\% = 0.9\Delta$	$+1.5\% = 0.7\Delta$	0
$C_{\mathrm{peak}}^{\phi\phi}$	-3.1%	$-2.2\% = -0.4\Delta$	$+8.2\% = 0.7\Delta$	$-3.1\% = 1.5\Delta$	$-0.2\% = -0.08\Delta$	$+3.2\% = 1\Delta$
$C_{\mathrm{peak}}^{\mathrm{TT,\ EISW}}$	$+16.0\%$	0	$-15.8\% = -1.3\Delta$	$-3.0\% = -1.5\Delta$	$+0.1\% = 0.05\Delta$	$+3.2\% = 1\Delta$

TABLE II. The fractional change to the quantities in the first column produced by respectively adding the EDE or varying the ΛCDM parameter from the ΛCDM model to the EDE model. Δ stands for the fractional change of the parameters x: $\Delta = (x_{\mathrm{EDE}} - x_{\Lambda\mathrm{CDM}})/x$.

where the matter-radiation equality $\ell_s^{\mathrm{eq}} \simeq 223$ [17]. I do not use ℓ_s^{eq} directly below because it cannot fully capture the effects of EDE.

- CMB lensing will smooth the peak and increase the small-scale power, which is the dominant contribution at very small scales. I use the peak of the power spectrum of the lensing potential $C_{\mathrm{peak}}^{\phi\phi}$ to characterize the strength of this effect.

- The early integrated Sachs–Wolfe (EISW) effect [80] is important for the scale around and larger than the first acoustic peak. Even at the last scattering surface, it is not completely matter-dominated, and the radiation is still causing the potential to decay. As a result, the energy of the photon at the corresponding scale is altered. I use the peak of the TT power spectrum contributed solely from the EISW effect $C_{\mathrm{peak}}^{\mathrm{TT,\ EISW}}$ to characterize it. Actually, it has been found both ΛCDM and the EDE model can lead to a consistent EISW effect [81].

In Table II, I show the effect of different components/parameters on these quantities by changing these components/parameters from the ΛCDM best fit to the AdS-EDE best fit, respectively.

Regardless of the implementation, all the EDE models provide a higher background expansion rate $H(z)$ in a period before and around the recombination, which leads to a smaller sound horizon r_s^*. Since the EDE itself does not significantly alter the late expansion history, the angular distance D_A to the last scattering surface is unchanged, which leads to a reduction in the angular separation of acoustic peaks $\theta_s^* = r_s^*/D_A$. Therefore, the project
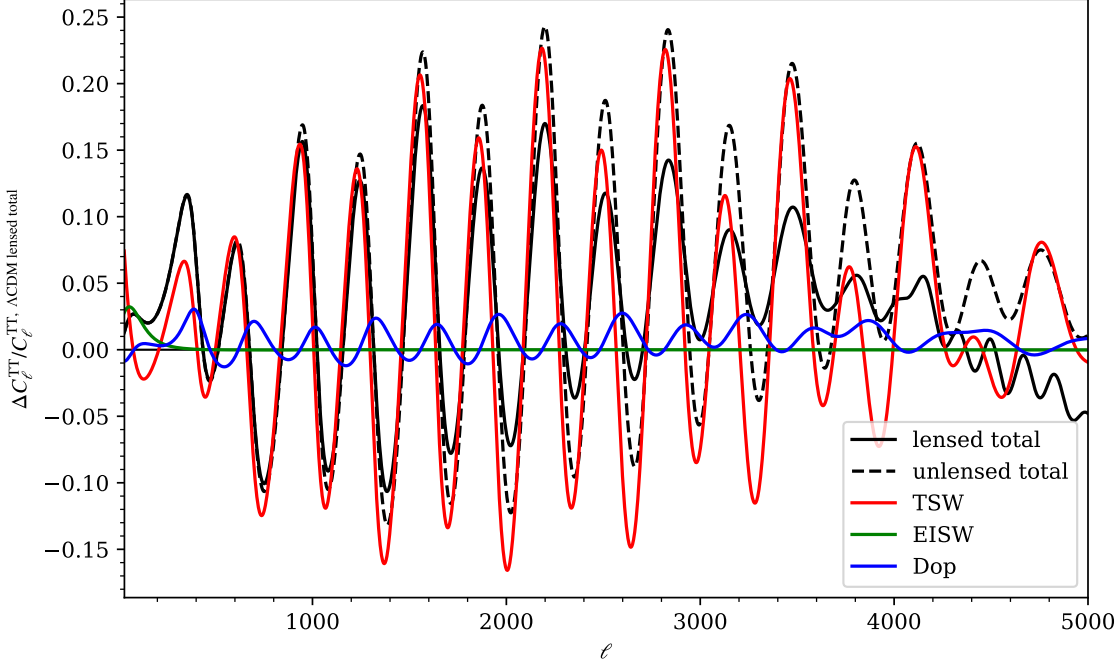
FIG. 1. The effect on the TT power spectrum of adding the EDE (the best-fit value of the EDE model) to the best-fit ΛCDM model. The colored lines are the effect on the unlensed TT spectrum where only a certain contribution is considered. "TSW" means intrinsic temperature corrected by Sachs-Wolfe, i.e. the contribution that comes from the difference between the potential at horizon crossing and today. "EISW" means early ISW effect, as explained above. And "Dop" means the Doppler effect, i.e. the contribution from Doppler shifts due to out-of-phase oscillations of the fluid with respect to temperature., which can be seen from the figure that it is always a minor contribution compared to TSW and EISW.

sound horizon $\ell_s \sim \pi/\theta_s^*$ is increased, which means the shift of the sound peak in the power spectrum. This leads to the most significant oscillating residuals in Figure 1.

Meanwhile, the higher expansion rate $H(z)$ around the recombination also reduces the diffusion damping scale r_D. Similarly, $\theta_D = r_D/D_A$ is reduced and $\ell_D \sim \pi/\theta_D$ is raised. Therefore, the diffusion damping is suppressed and the amplitude of the CMB spectrum at high ℓ is raised.

Another implication of the higher expansion rate $H(z)$ is a faster decay of the Weyl potential since EDE accelerates the expansion of the early universe at a period before recombina-
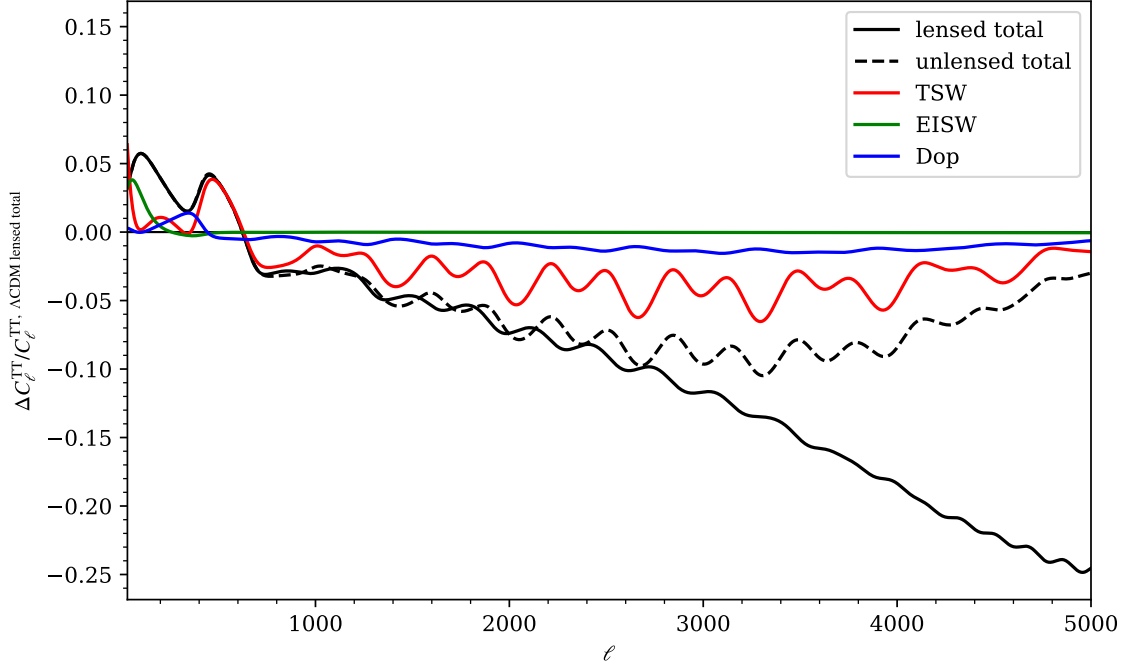
FIG. 2. Similar to Figure 1, but fixed θ_s^* by raising H_0.

tion and we will get a shallower Weyl potential eventually, see e.g. figures in [29, 42, 65, 82]. It affects the CMB power spectrum through three effects. The first two are the enhanced "potential envelope" and the early ISW effect as they arise from the decay of the potential, which is enhanced in the case of EDE. As a result, the $\mathrm{PH}_1/\mathrm{PH}_2$ and $C_{\mathrm{peak}}^{\mathrm{TT,\ EISW}}$ gets higher. On the other hand, a shallower Weyl potential also implies a lower matter power spectrum in the late universe. This also means that the lensing effect is weaker in the CMB TT power spectrum. In particular, it significantly reduces the amplitude at very high ℓ where CMB lensing is the dominant effect.

When we fit the EDE model to CMB observations, the other parameters will be shifted to reconcile the CMB power spectrum. Since we know that the ΛCDM model explains the observed CMB power spectrum well, we usually expect that by shifting the parameters, the EDE model produces a power spectrum similar to that of the ΛCDM model. However, this may not always be true since we have actually found that for some combinations of CMB datasets, the EDE model can fit the observations better than the ΛCDM model
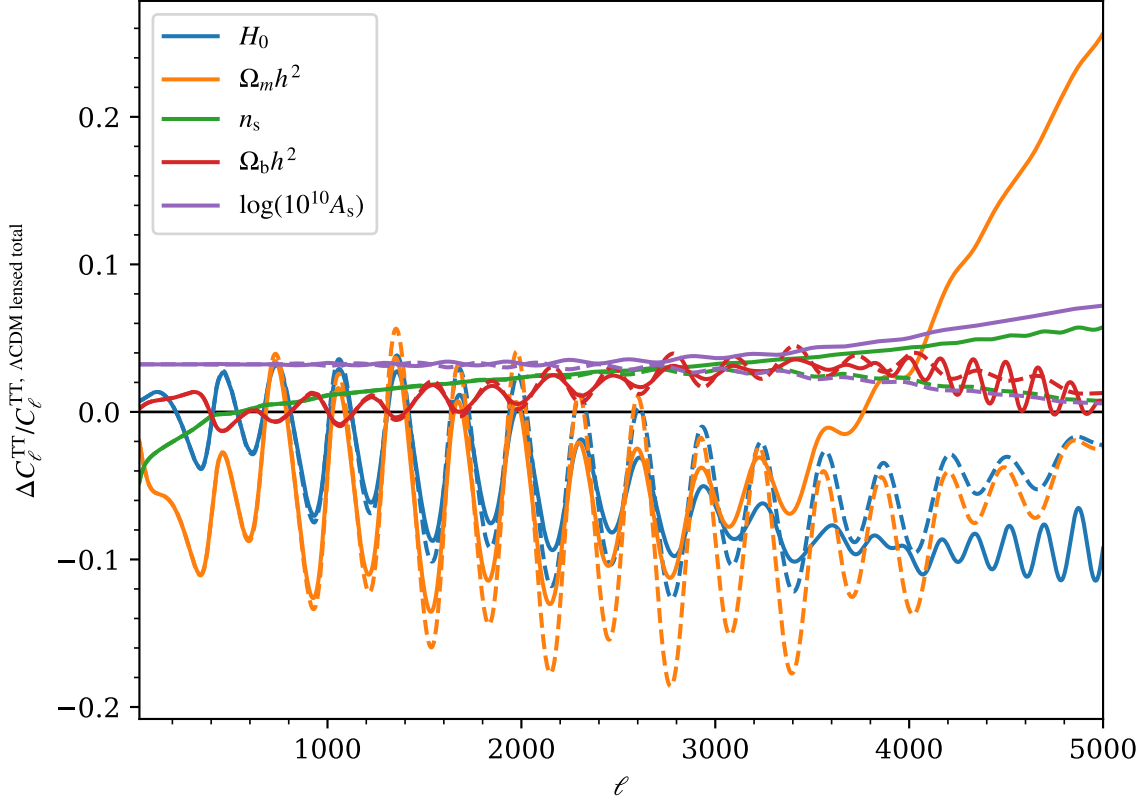
8

FIG. 3. The effect on the TT power spectrum of varying the ΛCDM parameter from the ΛCDM model to the EDE model respectively. The solid lines show the effect on the lensed spectrum while the dashed lines show the effect on the unlensed spectrum.

(e.g. [45, 65, 83–88]). [3] Nevertheless, we still assume in this section that the EDE model tries to fit a ΛCDM-like power spectrum because it is not yet clear whether this preference from CMB for the EDE model is general.

The most obviously shifted parameter is H_0, as it will reconcile the residuals due to the significant acoustic peak shift by changing the angular distance

$$D_A = 2998\,\mathrm{Mpc} \times \int \frac{\mathrm{d}z}{\sqrt{\omega_m(1+z)^3 + (H_0^2 - \omega_m)}}\,. \tag{3}$$

This is the direct reason why the Hubble tension has been relieved. It simultaneously

---

[3] However, for some CMB datasets, the EDE model may not fit the CMB observations better than the ΛCDM model if the local H_0 measurements are not fitted simultaneously, especially given the number of parameters added by EDE (e.g. [89]).

increases θ_s^* and θ_D. A large H_0 also reduced the lensing effect, partly due to the reduction in the distance the light travels after deflection and the change in the k-L projection relation.

Another parameter that can significantly affect the positions of the acoustic peaks is ω_m, which can change θ_s^* by affecting the acoustic horizon $\delta r_s^*/r_s^* \sim 1/4 \, \delta\omega_m/\omega_m$. However, as shown in Equation 3, it will also reduce D_A and finally result in a larger θ_s^*. Its effect on θ_D is similar but weaker, which can be clearly seen in Figure 2. Meanwhile, the reduced decay of Weyl potential, as opposed to the EDE (but with a different level of response), also helps reduce the "potential envelope" and the early ISW effect. These effects result in a lower PH_1/PH_2. Finally, a larger growth of matter perturbations leads to a stronger lensing effect. In some work, it was argued that BAO and uncalibrated SNeIa can constrain Ω_m because the late universe is still ΛCDM, and thus ω_m is lifted with H_0 [17, 63, 90–93]. In this work, I do not rely on this point as I only consider the CMB power spectrum. However, it is interesting that the present constraints on the EDE model obtained a Ω_m consistent with the results of BAO and uncalibrated SNeIa. We will see in the next section that this may be a coincidence due to the weak observation constraints currently (see also Figure 6 of Ref.[64]).

A large ω_b can reduce both the sound horizon and the diffusion damping scale (but it's more effective for the latter), leading to lower θ_s^* and θ_D. The main effect of ω_b is altering the zero-point of the acoustic oscillations, resulting in a higher PH_1/PH_2.

There are three reasons cause the raise of n_s. Firstly, although n_s does not affect θ_D, It provides greater amplitude at small scales, thus counteracting the enhanced diffusion damping [17, 65, 82, 94]. This is required because the effect of the EDE on θ_s^* and θ_D is unbalanced, whereas shifts in the other parameters will either only change them equally or have very little effect. Secondly, n_s can directly balance PH_1/PH_2 [94]. Thirdly, n_s will reduce the peak of the matter power spectrum as its scale is smaller than the pivot scale. However, n_s enhances $C_L^{\phi\phi}$ at high L, which can help to transfer higher power from large $(\ell-L)$ to small (ℓ) scales. Therefore, the amplitude at the very high ℓ becomes higher instead to balance the effect of EDE. Besides, $C_{\text{peak}}^{\text{TT, EISW}}$ gets lower as its scale is also smaller than the pivot scale. Actually, an interesting fact is that if H_0 were to reconcile with the result of SH0ES, we would probably need a Harrison-Zeldovich spectrum $n_s = 1$ [65, 86, 88, 94–98], which has a great impact on the inflation model (e.g. Refs. [99, 100]).

Finally, the role of $A_s \exp(-2\tau)$ is simple. It directly changes the overall amplitude of

the unlensed TT power spectrum and the lensing potential spectrum (since I vary A_s here). The latter leads to the further enhancement of the lensed TT power spectrum at very high ℓ. On the other hand, if one chooses to vary τ, there is only the former effect.

III.   SCALE-DEPENDENT ΛCDM PARAMETERS INFERRED FROM THE CMB

While the effects of the component/parameter shifts mentioned above can in practice allow the EDE model to fit the CMB observations similar to ΛCDM, this is most likely a coincidence due to the current lack of observational precision as well as the limited range of scales. Here are three main reasons why the degeneration of these two models cannot be satisfied at all scales:

- The effect of EDE on the Weyl potential is not trivial, and it cannot be balanced simply by varying ω_m. Therefore, scale-dependent "potential envelope" and EISW effect differences must exist between EDE and ΛCDM. This was brought up in Ref.[17], where they also suspected it may be related to the high-low ℓ inconsistencies [49, 50] and the lensing anomaly [10, 49, 51, 52] in the Planck 2018 data. However, the lensing anomaly seems to be not related to EDE [65, 101] and the lensing anomaly is reduced in the updated PR4 data [70, 102]. On the other hand, the evolution of the Weyl potential is closely related to the details of the EDE model. Hence I will not rely on this point here.

- In the above, I used 5 quantities to characterize the CMB TT power spectrum. Even considering the compressed information, ΛCDM model has fewer free parameters [4]. Therefore it is not possible that all quantities can be well reconciled. Since these quantities are important at different scales, its back effect is the variation of ΛCDM parameters at different scales.

- Another important source of scale dependence is similar effects in the power spectrum but with different shapes as functions of scale, which I will elaborate on below.

I assume that the real universe is ΛCDM or AdS-EDE with parameter values as in Table I, and generate mock data using `cobaya_mock_cmb`[5][103] for a CMB-S4-like observation. Then

---

[4] $A_s \exp(-2\tau)$ is used to absorb the overall amplitude which is not mentioned above, while, as stated below, I consider the information from the polarization spectrum for τ.

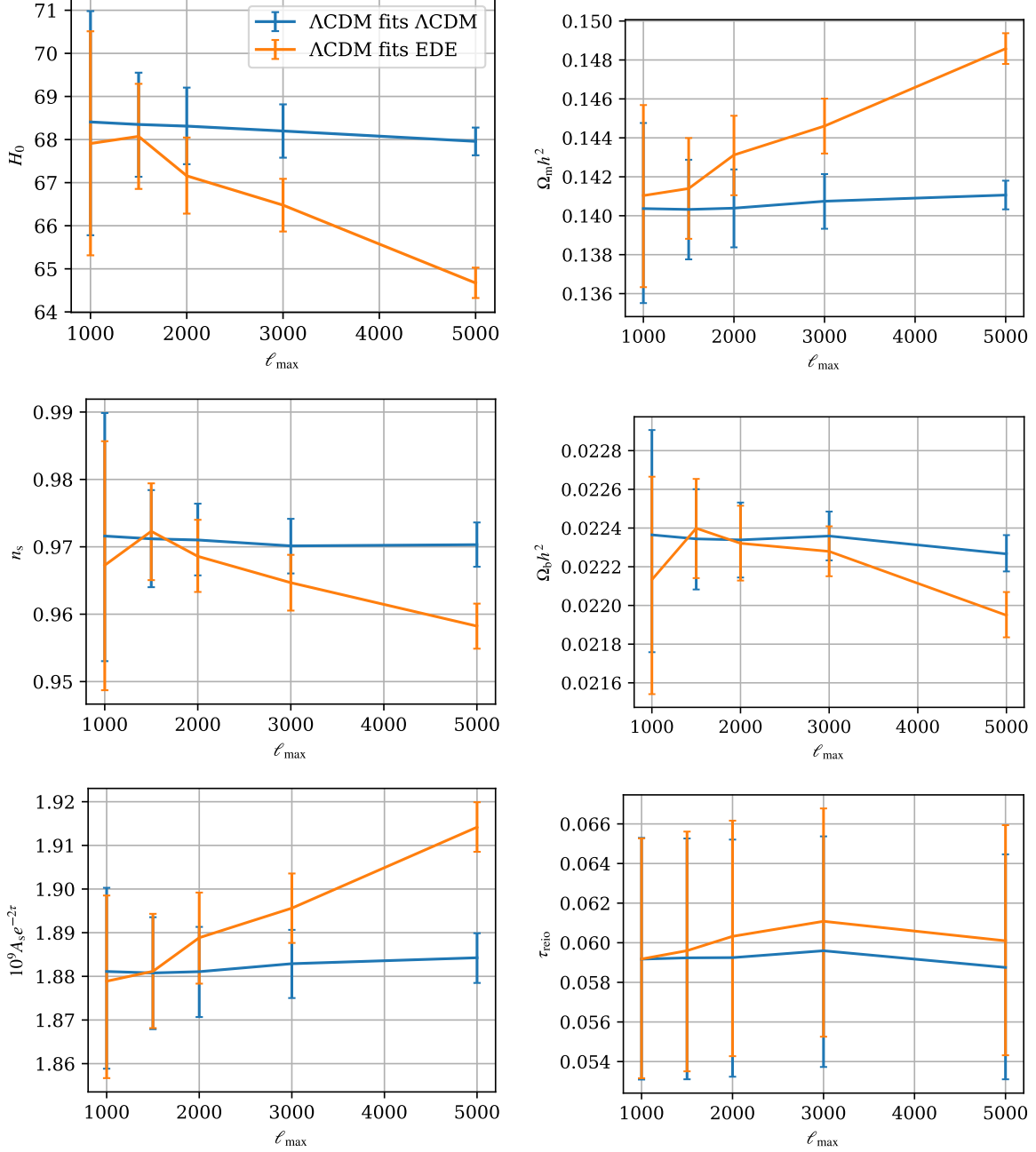[5] `https://github.com/misharash/cobaya_mock_cmb`. I used the `deproj0` noise curves.

FIG. 4. The posterior distribution of ΛCDM parameters inferred from mock CMB data with different cut-off $\ell_{\max}$. The error bars show the mean and 68% confidence intervals.

I fit these two mock data till some $\ell_{\max}$ respectively with the ΛCDM model. Only the TT power spectrum is used, so I impose a prior for τ from the previously mentioned ΛCDM fit the current observation [6]. I used `nautilus` [104] for importance nested sampling accelerated

---

[6] While this may in principle introduce a bias for the case of EDE as mock data, it can be seen from the posterior of τ in Figure 4 that τ does not have a significant effect.
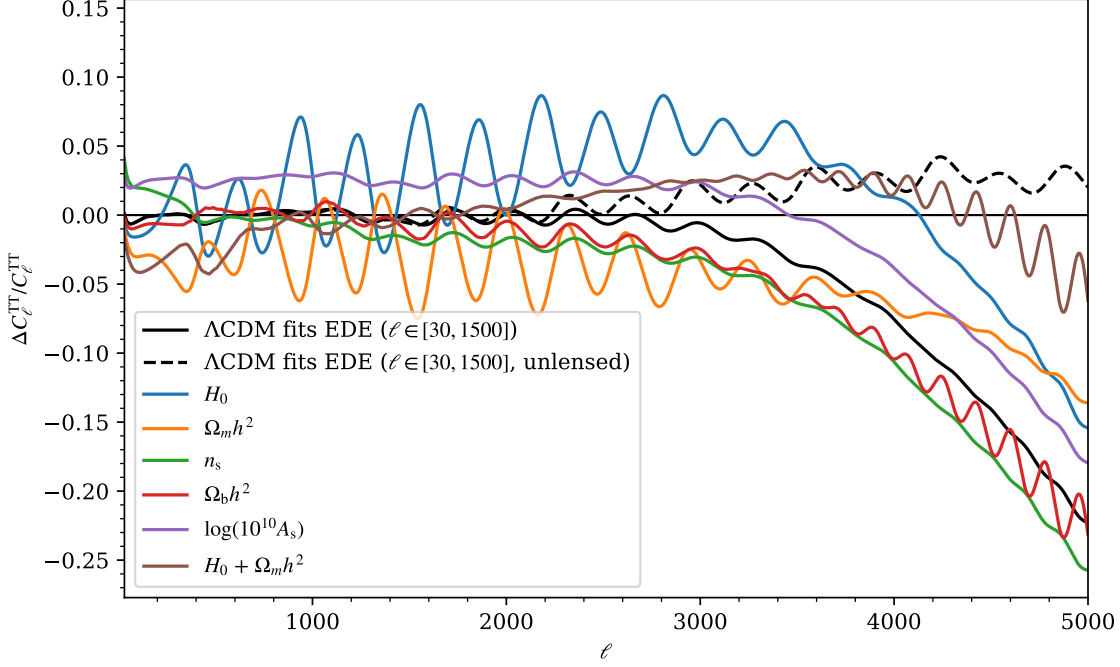
FIG. 5. The black lines are the residual at the best-fit ΛCDM point ($\ell \in [30, 1500]$) of the TT power spectrum compared to mock data (EDE). The colored lines are the residuals after varying the parameters from the best-fit values of $\ell \in [30, 1500]$ to the best-fit values of $\ell \in [30, 5000]$, respectively. They are the residuals between lensed power spectrums when not stated.

with machine learning. The trends of the posterior distributions of the ΛCDM parameters varying with $\ell_{\max}$ are shown in Figure 4.

We can find that the posterior distribution of $\ell_{\max} \lesssim 1500$ is similar for both cases. This is understandable, since the values of the mock data are taken from current observations on the same CMB, and the main constraining power of the current observations is at these scales. When ΛCDM is used to fit a ΛCDM universe, there is no observable scale dependence of the parameters, which verifies that our pipeline has no bias. In contrast, when ΛCDM is used to fit an EDE universe, the ΛCDM parameters, except τ, produce a significant scale-dependent shift. The largest shift lies between the full range ($\ell_{\max} = 5000$) and $\ell_{\max} \sim 1500$, where the parameters have a shift of about $1 \sim 2\,\sigma$.

To understand these behaviors, I show in Figure 5 the residuals of $\ell_{\max} = 1500$ relative to the EDE mock data, and how the ΛCDM parameters shift to affect the residuals sep-

arately. Firstly, at high ℓ, ΛCDM has positive unlensed residuals, which is, in part, due to the mismatch between the primordial power spectrum as a power-law spectrum and the exponential suppression of the diffusion damping. The fractional change to the unlensed TT power spectrum due to n_s is proportional to $\ln(\ell/\ell_{\mathrm{pivot}})$, while for θ_D, it $\propto -\ell^2$. Hence, even if they can cancel out at low ℓ, they will inevitably diverge at high ℓ. This effect may be observable if we can delensing efficiently. However, at very high ℓ, the transfer from large to small scales due to CMB lensing is the dominant effect. In Figure 3, we can see that a large ω_m will induce a dramatic enhancement of the lensed TT spectrum at very high ℓ. When ΛCDM only fits the part of $\ell < 1500$, this effect is ignored and the constraints on ω_m will come mainly from the "potential envelope" and EISW effects, which favor a low ω_m due to the lack of EDE to produce a shallower Weyl potential. As a result, this leads to large negative residuals in the unfitted part. Actually, this is visible in the residuals of some EDE fits to the real observations (e.g. Figure 12 of Ref.[64], where instead the residuals of EDE relative to ΛCDM are shown.).

When $\ell_{\max}$ moves to small scales, ω_m increases and H_0 decreases to compensate for the lensing effect. At the same time, they maintain their relation to preserve the acoustic peak separation. Their net effects, shown as brown lines, are negative residuals at large scales and positive residuals at $2000 \lesssim \ell \lesssim 4000$. The former, due to the reduced "potential envelope" and EISW effects, can be compensated by increasing the primordial power spectrum (lowering n_s and increasing A_s). The lower n_s simultaneously mitigates the positive residuals at $2000 \lesssim \ell \lesssim 4000$, while the enhancement of diffusion damping by lowering ω_b has a similar effect.

Moreover, since the parameters derived from the analysis using the full scale have large departures from $\ell_{\max} \sim 1500$, whose results are similar to the current observations, the parameters based on the full-scale analysis will deviate from the current observations. For example, the full-scale analysis finds $\Omega_m = 0.355 \pm 0.006$, which conflicts with the current BAO and SNeIa measurements. Meanwhile, it finds $\omega_b = 0.0219 \pm 0.0001$, lower than the current constraint determined from BBN.

IV. CONCLUSION

I analyzed the phenomenology for general EDE and parameters of ΛCDM. I've found that because the effects of different components/parameters vary at different scales, it's not possible to keep ΛCDM degenerate with EDE at all scales. Consequently, if the real universe is as described by the EDE model, then when we use ΛCDM to fit it, we will find that its parameters are scale-dependent. Here I use the CMB-S4 observation on the TT power spectrum (with a prior on τ from the current observations) as an example to test this behavior. As the range of the analysis increases from $\ell_{\max} \sim 1500$ to small scales, H_0, n_s, and ω_b decreases, while ω_m and $A_s e^{-2\tau}$ increases. Actually, if there is some evidence for non-zero parameters used to quantify the running of these parameters, such as the running of scalar spectral index α_s, it could also be a sign of EDE. The main reason for this scale dependence is that variations in the Weyl potential by the EDE will cause different effects between low ℓ and very high ℓ.

Therefore, if the constraints on the ΛCDM parameters in future CMB observations, e.g., CMB-S4 [105], Simons Observatory [106], show the same scale-dependent shift direction at $\ell \gtrsim 1500$ as predicted here, then this is a possible signal for the EDE model as a solution to the Hubble tension. Meanwhile, this hint relies on the phenomenology shared by the EDE models without delving into the differences between the EDE models, making it an important addition to the direct fitting of specific EDE models. Moreover, my results also imply that if the real universe is as described by the EDE, some observables inferred from future CMB observations (assuming ΛCDM) will be in conflict with other observations. For example, a very large Ω_m could conflict with BAO and SNeIa observation which are independent from the early Universe. Meanwhile, the constraints for ω_b are lower than those from BBN. These suggest that new tensions may arise.

Appendix A: Scale-dependent ΛCDM parameters with various mock ADE models

Here, I investigate the universality of the above conclusion for the EDE model through various Acoustic Dark Energy (ADE) models [29]. In the ADE model, EDE is simulated as a perfect fluid. The equation of state of ADE is modeled as:

$$1 + w(a) = \frac{1 + w_f}{[1 + (a_c/a)^{3(1+w_f)/p}]^p}. \tag{A1}$$

Around the critical scale factor a_c, w transitions from -1 to w_f, and the rapidity of the transition is controlled by p. The fractional energy density of ADE at a_c is denoted as f_{EDE}. In addition, there is another adjustable parameter, which is the sound speed c_s^2 of the ADE. With these five parameters, ADE can mimic the behavior of many other EDE models, especially in terms of the background dynamics of interest here. For example, the AdS-EDE model tested above corresponds to $c_s^2 = 1$ and has $w_f \gtrsim 1$ in the AdS phase. The axion-like EDE model ($n = 3$) has $w_f = 1/2$, $p = 1$, and $c_s^2 \in [1/2, 1]$. The canonical ADE in Ref.[29] has $w_f = 1$ and $c_s^2 = 1$ fixed.

I selected a toy ADE model ($z_c = 3400, c_s^2 = 0.75, p = 1, w_f = 0.75$) as the fiducial model, and then for each ADE parameter, I varied it within a reasonable range to evaluate its impact on the conclusion mentioned above, namely, the scale dependence of the ΛCDM parameters inferred from the CMB. The range for each parameter is as follows:

$$z_c = [3000, 4000] \tag{A2}$$

$$c_s^2 = [0.5, 1] \tag{A3}$$

$$p = [0.5, 2] \tag{A4}$$

$$w_f = [0.5, 1] \tag{A5}$$

The ADE fractional energy density f_{EDE} at z_c is always fixed at 0.1, because the effect of EDE should be simply proportional to f_{EDE} at leading order. It is important to note that the ADE's f_{EDE} is not equal to the peak value of $f_{\mathrm{EDE}}(z)$, so its specific value should not be directly compared with f_{EDE} in other EDE models. At the same time, other ADE parameters also affect the relationship between f_{EDE} and the peak value of $f_{\mathrm{EDE}}(z)$ (especially the parameter p), so they also influence the strength of the ADE effect. As a result, only the direction of the parameter shifts should be compared, rather than the magnitude of the
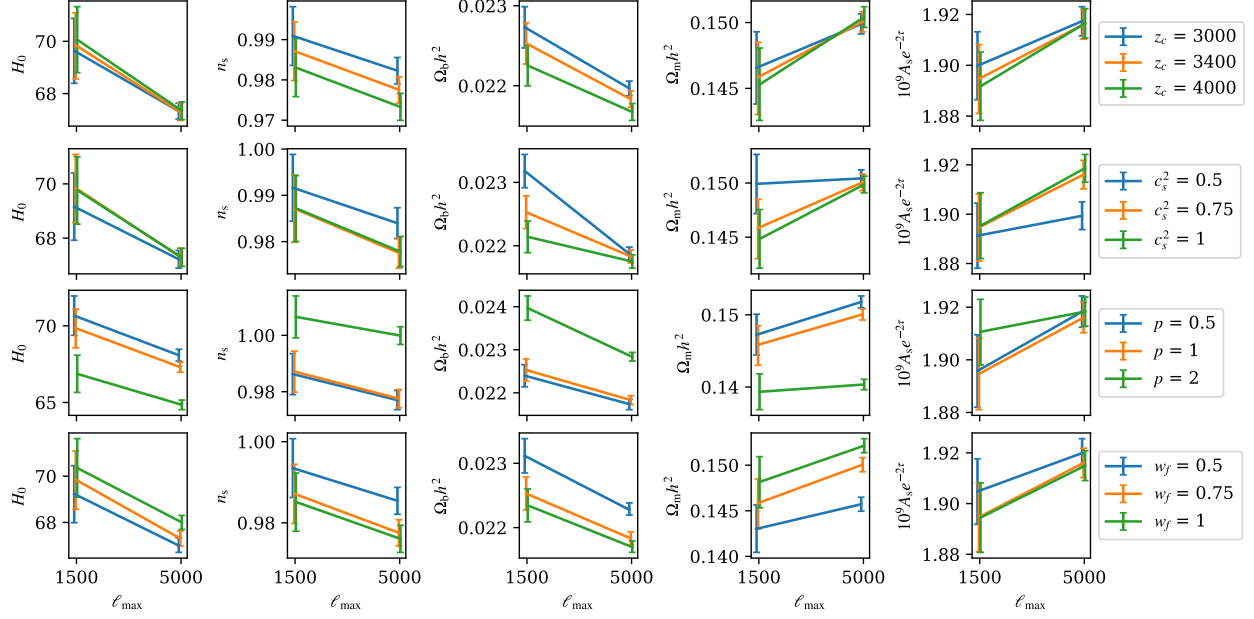
16

FIG. 6. The posterior distribution of the ΛCDM parameters inferred from mock CMB data with different cut-off $\ell_{\max}$. For each row, the assumed mock data is generated by altering one parameter based on the fiducial ADE model ($z_c = 3400$, $c_s^2 = 0.75$, $p = 1$, $w_f = 0.75$) as shown in the legend on the right. The error bars show the mean and 68% confidence intervals.

shifts. The other cosmological parameters are fixed as follows:

$$H_0 = 73.04, \ n_s = 1, \ \Omega_b h^2 = 0.02218, \ \Omega_m = 0.3, \ \ln\left(10^{10} A_s\right) = 3.08, \ \tau = 0.055\,. \tag{A6}$$

The results of the parameter shifts are shown in Figure 6, which demonstrate that the decrease in H_0, n_s, and $\omega_b h^2$ with increasing $\ell_{\max}$ is sufficiently robust with respect to various ADE parameters. For the parameters ω_m and $A_s e^{-2\tau}$, although the shifts in the parameters are not as pronounced in some edge cases, the direction of the shifts remains consistent with the original conclusion.

Appendix B: Scale-dependent ΛCDM parameters inferred from the CMB including the polarization spectrum

In Figure 7, I present the results with the inclusion of the polarization spectrum in the fitting, where the conclusion changes, and $\omega_b h^2$ increases with $\ell_{\max}$ instead. This is understandable because the above analysis was conducted with respect to the temperature
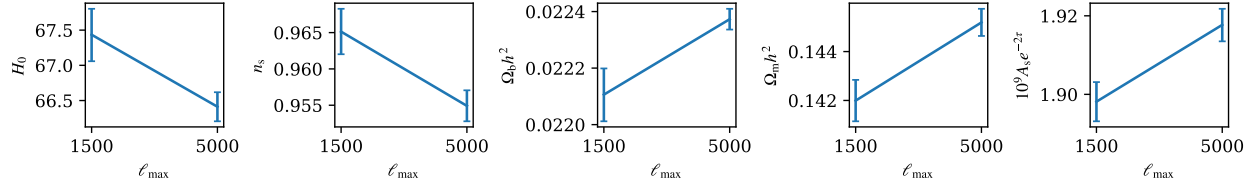
FIG. 7. The posterior distribution of the ΛCDM parameters inferred from mock CMB data with different cut-off $\ell_{\max}$. The mock model is the same as the one used in Figure 4 but the polarization spectrum (TE, EE) is also included in the mock CMB data. The error bars show the mean and 68% confidence intervals.

spectrum. Since different EDE models exhibit significant differences in the polarization spectrum, the trends shown here may not be applicable to all EDE models.

[1] L. Verde, T. Treu, and A. G. Riess, Tensions between the Early and the Late Universe, Nature Astron. **3**, 891 (2019), arXiv:1907.10625 [astro-ph.CO].

[2] E. Di Valentino, O. Mena, S. Pan, L. Visinelli, W. Yang, A. Melchiorri, D. F. Mota, A. G. Riess, and J. Silk, In the realm of the Hubble tension—a review of solutions, Class. Quant. Grav. **38**, 153001 (2021), arXiv:2103.01183 [astro-ph.CO].

[3] L. Perivolaropoulos and F. Skara, Challenges for ΛCDM: An update, New Astron. Rev. **95**, 101659 (2022), arXiv:2105.05208 [astro-ph.CO].

[4] N. Schöneberg, G. Franco Abellán, A. Pérez Sánchez, S. J. Witte, V. Poulin, and J. Lesgourgues, The H0 Olympics: A fair ranking of proposed models, Phys. Rept. **984**, 1 (2022), arXiv:2107.10291 [astro-ph.CO].

[5] P. Shah, P. Lemos, and O. Lahav, A buyer's guide to the Hubble constant, Astron. Astrophys. Rev. **29**, 9 (2021), arXiv:2109.01161 [astro-ph.CO].

[6] E. Abdalla *et al.*, Cosmology intertwined: A review of the particle physics, astrophysics, and cosmology associated with the cosmological tensions and anomalies, JHEAp **34**, 49 (2022), arXiv:2203.06142 [astro-ph.CO].

[7] E. Di Valentino, Challenges of the Standard Cosmological Model, Universe **8**, 399 (2022).

[8] J.-P. Hu and F.-Y. Wang, Hubble Tension: The Evidence of New Physics, Universe **9**, 94 (2023), arXiv:2302.05709 [astro-ph.CO].

[9] L. Verde, N. Schöneberg, and H. Gil-Marín, A tale of many H_0, (2023), arXiv:2311.13305 [astro-ph.CO].

[10] N. Aghanim *et al.* (Planck), Planck 2018 results. VI. Cosmological parameters, Astron. Astrophys. **641**, A6 (2020), [Erratum: Astron.Astrophys. 652, C4 (2021)], arXiv:1807.06209 [astro-ph.CO].

[11] A. G. Riess *et al.*, A Comprehensive Measurement of the Local Value of the Hubble Constant with 1 km s^{-1} Mpc^{-1} Uncertainty from the Hubble Space Telescope and the SH0ES Team, Astrophys. J. Lett. **934**, L7 (2022), arXiv:2112.04510 [astro-ph.CO].

[12] J. L. Bernal, L. Verde, and A. G. Riess, The trouble with H_0, JCAP **10**, 019, arXiv:1607.05617 [astro-ph.CO].

[13] G. E. Addison, D. J. Watts, C. L. Bennett, M. Halpern, G. Hinshaw, and J. L. Weiland, Elucidating ΛCDM: Impact of Baryon Acoustic Oscillation Measurements on the Hubble Constant Discrepancy, Astrophys. J. **853**, 119 (2018), arXiv:1707.06547 [astro-ph.CO].

[14] P. Lemos, E. Lee, G. Efstathiou, and S. Gratton, Model independent $H(z)$ reconstruction using the cosmic inverse distance ladder, Mon. Not. Roy. Astron. Soc. **483**, 4803 (2019), arXiv:1806.06781 [astro-ph.CO].

[15] K. Aylor, M. Joy, L. Knox, M. Millea, S. Raghunathan, and W. L. K. Wu, Sounds Discordant: Classical Distance Ladder & ΛCDM -based Determinations of the Cosmological Sound Horizon, Astrophys. J. **874**, 4 (2019), arXiv:1811.00537 [astro-ph.CO].

[16] N. Schöneberg, J. Lesgourgues, and D. C. Hooper, The BAO+BBN take on the Hubble tension, JCAP **10**, 029, arXiv:1907.11594 [astro-ph.CO].

[17] L. Knox and M. Millea, Hubble constant hunter's guide, Phys. Rev. D **101**, 043533 (2020), arXiv:1908.03663 [astro-ph.CO].

[18] N. Arendse *et al.*, Cosmic dissonance: are new physics or systematics behind a short sound horizon?, Astron. Astrophys. **639**, A57 (2020), arXiv:1909.07986 [astro-ph.CO].

[19] G. Efstathiou, To H0 or not to H0?, Mon. Not. Roy. Astron. Soc. **505**, 3866 (2021), arXiv:2103.08723 [astro-ph.CO].

[20] C. Krishnan, R. Mohayaee, E. O. Colgáin, M. M. Sheikh-Jabbari, and L. Yin, Does Hubble tension signal a breakdown in FLRW cosmology?, Class. Quant. Grav. **38**, 184001 (2021), arXiv:2105.09790 [astro-ph.CO].

[21] R.-G. Cai, Z.-K. Guo, S.-J. Wang, W.-W. Yu, and Y. Zhou, No-go guide for the Hubble tension: Late-time solutions, Phys. Rev. D **105**, L021301 (2022), arXiv:2107.13286 [astro-ph.CO].

[22] R. E. Keeley and A. Shafieloo, Ruling Out New Physics at Low Redshift as a Solution to the H0 Tension, Phys. Rev. Lett. **131**, 111002 (2023), arXiv:2206.08440 [astro-ph.CO].

[23] A. Gómez-Valent, A. Favale, M. Migliaccio, and A. A. Sen, Late-time phenomenology required to solve the H0 tension in view of the cosmic ladders and the anisotropic and angular BAO datasets, Phys. Rev. D **109**, 023525 (2024), arXiv:2309.07795 [astro-ph.CO].

[24] J.-Q. Jiang, D. Pedrotti, S. S. da Costa, and S. Vagnozzi, Non-parametric late-time expansion history reconstruction and implications for the Hubble tension in light of DESI, (2024), arXiv:2408.02365 [astro-ph.CO].

[25] T. Karwal and M. Kamionkowski, Dark energy at early times, the Hubble parameter, and the string axiverse, Phys. Rev. D **94**, 103523 (2016), arXiv:1608.01309 [astro-ph.CO].

[26] V. Poulin, T. L. Smith, T. Karwal, and M. Kamionkowski, Early Dark Energy Can Resolve The Hubble Tension, Phys. Rev. Lett. **122**, 221301 (2019), arXiv:1811.04083 [astro-ph.CO].

[27] N. Kaloper, Dark energy, H_0 and weak gravity conjecture, Int. J. Mod. Phys. D **28**, 1944017 (2019), arXiv:1903.11676 [hep-th].

[28] P. Agrawal, F.-Y. Cyr-Racine, D. Pinner, and L. Randall, Rock 'n' roll solutions to the Hubble tension, Phys. Dark Univ. **42**, 101347 (2023), arXiv:1904.01016 [astro-ph.CO].

[29] M.-X. Lin, G. Benevento, W. Hu, and M. Raveri, Acoustic Dark Energy: Potential Conversion of the Hubble Tension, Phys. Rev. D **100**, 063542 (2019), arXiv:1905.12618 [astro-ph.CO].

[30] T. L. Smith, V. Poulin, and M. A. Amin, Oscillating scalar fields and the Hubble tension: a resolution with novel signatures, Phys. Rev. D **101**, 063523 (2020), arXiv:1908.06995 [astro-ph.CO].

[31] F. Niedermann and M. S. Sloth, New early dark energy, Phys. Rev. D **103**, L041303 (2021), arXiv:1910.10739 [astro-ph.CO].

[32] J. Sakstein and M. Trodden, Early Dark Energy from Massive Neutrinos as a Natural Resolution of the Hubble Tension, Phys. Rev. Lett. **124**, 161301 (2020), arXiv:1911.11760 [astro-ph.CO].

[33] G. Ye and Y.-S. Piao, Is the Hubble tension a hint of AdS phase around recombination?, Phys. Rev. D **101**, 083507 (2020), arXiv:2001.02451 [astro-ph.CO].

[34] A. Gogoi, R. K. Sharma, P. Chanda, and S. Das, Early Mass-varying Neutrino Dark Energy: Nugget Formation and Hubble Anomaly, Astrophys. J. **915**, 132 (2021), arXiv:2005.11889 [astro-ph.CO].

[35] M. Braglia, W. T. Emond, F. Finelli, A. E. Gumrukcuoglu, and K. Koyama, Unified framework for early dark energy from α-attractors, Phys. Rev. D **102**, 083513 (2020), arXiv:2005.14053 [astro-ph.CO].

[36] M.-X. Lin, W. Hu, and M. Raveri, Testing H_0 in Acoustic Dark Energy with Planck and ACT Polarization, Phys. Rev. D **102**, 123523 (2020), arXiv:2009.08974 [astro-ph.CO].

[37] S. D. Odintsov, D. Sáez-Chillón Gómez, and G. S. Sharov, Analyzing the H_0 tension in $F(R)$ gravity models, Nucl. Phys. B **966**, 115377 (2021), arXiv:2011.03957 [gr-qc].

[38] O. Seto and Y. Toda, Comparing early dark energy and extra radiation solutions to the Hubble tension with BBN, Phys. Rev. D **103**, 123501 (2021), arXiv:2101.03740 [astro-ph.CO].

[39] S. Nojiri, S. D. Odintsov, D. Saez-Chillon Gomez, and G. S. Sharov, Modeling and testing the equation of state for (Early) dark energy, Phys. Dark Univ. **32**, 100837 (2021), arXiv:2103.05304 [gr-qc].

[40] T. Karwal, M. Raveri, B. Jain, J. Khoury, and M. Trodden, Chameleon early dark energy and the Hubble tension, Phys. Rev. D **105**, 063535 (2022), arXiv:2106.13290 [astro-ph.CO].

[41] K. Rezazadeh, A. Ashoorioon, and D. Grin, Cascading Dark Energy, (2022), arXiv:2208.07631 [astro-ph.CO].

[42] V. Poulin, T. L. Smith, and T. Karwal, The Ups and Downs of Early Dark Energy solutions to the Hubble tension: A review of models, hints and constraints circa 2023, Phys. Dark Univ. **42**, 101348 (2023), arXiv:2302.09032 [astro-ph.CO].

[43] S. D. Odintsov, V. K. Oikonomou, and G. S. Sharov, Early dark energy with power-law F(R) gravity, Phys. Lett. B **843**, 137988 (2023), arXiv:2305.17513 [gr-qc].

[44] S. Vagnozzi, Seven Hints That Early-Time New Physics Alone Is Not Sufficient to Solve the Hubble Tension, Universe **9**, 393 (2023), arXiv:2308.16628 [astro-ph.CO].

[45] V. Poulin, T. L. Smith, and A. Bartlett, Dark energy at early times and ACT data: A larger Hubble constant without late-time priors, Phys. Rev. D **104**, 123550 (2021), arXiv:2109.06229 [astro-ph.CO].

[46] G. S. Farren, O. H. E. Philcox, and B. D. Sherwin, Determining the Hubble constant without the sound horizon: Perspectives with future galaxy surveys, Phys. Rev. D **105**, 063503 (2022),

arXiv:2112.10749 [astro-ph.CO].

[47] S. Brieden, H. Gil-Marín, and L. Verde, A tale of two (or more) h's, JCAP **04**, 023, arXiv:2212.04522 [astro-ph.CO].

[48] O. Akarsu, E. O. Colgáin, A. A. Sen, and M. M. Sheikh-Jabbari, ΛCDM Tensions: Localising Missing Physics through Consistency Checks, Universe **10**, 305 (2024), arXiv:2402.04767 [astro-ph.CO].

[49] G. E. Addison, Y. Huang, D. J. Watts, C. L. Bennett, M. Halpern, G. Hinshaw, and J. L. Weiland, Quantifying discordance in the 2015 Planck CMB spectrum, Astrophys. J. **818**, 132 (2016), arXiv:1511.00055 [astro-ph.CO].

[50] N. Aghanim *et al.* (Planck), Planck intermediate results. LI. Features in the cosmic microwave background temperature power spectrum and shifts in cosmological parameters, Astron. Astrophys. **607**, A95 (2017), arXiv:1608.02487 [astro-ph.CO].

[51] P. Motloch and W. Hu, Lensinglike tensions in the *Planck* legacy release, Phys. Rev. D **101**, 083515 (2020), arXiv:1912.06601 [astro-ph.CO].

[52] P. Motloch and W. Hu, Tensions between direct measurements of the lens power spectrum from Planck data, Phys. Rev. D **97**, 103536 (2018), arXiv:1803.11526 [astro-ph.CO].

[53] E. Di Valentino, A. Melchiorri, and J. Silk, Cosmological constraints in extended parameter space from the Planck 2018 Legacy release, JCAP **01**, 013, arXiv:1908.01391 [astro-ph.CO].

[54] E. Di Valentino, A. Melchiorri, and J. Silk, Investigating Cosmic Discordance, Astrophys. J. Lett. **908**, L9 (2021), arXiv:2003.04935 [astro-ph.CO].

[55] S. Aiola *et al.* (ACT), The Atacama Cosmology Telescope: DR4 Maps and Cosmological Parameters, JCAP **12**, 047, arXiv:2007.07288 [astro-ph.CO].

[56] L. Balkenhol *et al.* (SPT-3G), Constraints on ΛCDM extensions from the SPT-3G 2018 EE and TE power spectra, Phys. Rev. D **104**, 083509 (2021), arXiv:2103.13618 [astro-ph.CO].

[57] L. Balkenhol *et al.* (SPT-3G), Measurement of the CMB temperature power spectrum and constraints on cosmology from the SPT-3G 2018 TT, TE, and EE dataset, Phys. Rev. D **108**, 023510 (2023), arXiv:2212.05642 [astro-ph.CO].

[58] W. Handley and P. Lemos, Quantifying the global parameter tensions between ACT, SPT and Planck, Phys. Rev. D **103**, 063529 (2021), arXiv:2007.08496 [astro-ph.CO].

[59] E. Di Valentino, W. Giarè, A. Melchiorri, and J. Silk, Quantifying the global 'CMB tension' between the Atacama Cosmology Telescope and the Planck satellite in extended models of

cosmology, Mon. Not. Roy. Astron. Soc. **520**, 210 (2023), arXiv:2209.14054 [astro-ph.CO].

[60] M. Forconi, W. Giarè, E. Di Valentino, and A. Melchiorri, Cosmological constraints on slow roll inflation: An update, Phys. Rev. D **104**, 103528 (2021), arXiv:2110.01695 [astro-ph.CO].

[61] W. Giarè, F. Renzi, O. Mena, E. Di Valentino, and A. Melchiorri, Is the Harrison-Zel'dovich spectrum coming back? ACT preference for ns $\sim$ 1 and its discordance with Planck, Mon. Not. Roy. Astron. Soc. **521**, 2911 (2023), arXiv:2210.09018 [astro-ph.CO].

[62] E. Di Valentino, W. Giarè, A. Melchiorri, and J. Silk, Health checkup test of the standard cosmological model in view of recent cosmic microwave background anisotropies experiments, Phys. Rev. D **106**, 103506 (2022), arXiv:2209.12872 [astro-ph.CO].

[63] G. Ye and Y.-S. Piao, T_0 censorship of early dark energy and AdS vacua, Phys. Rev. D **102**, 083523 (2020), arXiv:2008.10832 [astro-ph.CO].

[64] J.-Q. Jiang and Y.-S. Piao, Testing AdS early dark energy with Planck, SPTpol, and LSS data, Phys. Rev. D **104**, 103524 (2021), arXiv:2107.07128 [astro-ph.CO].

[65] J.-Q. Jiang and Y.-S. Piao, Toward early dark energy and ns=1 with Planck, ACT, and SPT observations, Phys. Rev. D **105**, 103514 (2022), arXiv:2202.13379 [astro-ph.CO].

[66] N. Aghanim *et al.* (Planck), Planck 2018 results. V. CMB power spectra and likelihoods, Astron. Astrophys. **641**, A5 (2020), arXiv:1907.12875 [astro-ph.CO].

[67] S. Hamimeche and A. Lewis, Likelihood Analysis of CMB Temperature and Polarization Power Spectra, Phys. Rev. D **77**, 103013 (2008), arXiv:0801.0554 [astro-ph].

[68] A. Mangilli, S. Plaszczynski, and M. Tristram, Large-scale cosmic microwave background temperature and polarization cross-spectra likelihoods, Mon. Not. Roy. Astron. Soc. **453**, 3174 (2015), arXiv:1503.01347 [astro-ph.CO].

[69] M. Tristram *et al.*, Planck constraints on the tensor-to-scalar ratio, Astron. Astrophys. **647**, A128 (2021), arXiv:2010.01139 [astro-ph.CO].

[70] E. Rosenberg, S. Gratton, and G. Efstathiou, CMB power spectra and cosmological parameters from Planck PR4 with CamSpec, Mon. Not. Roy. Astron. Soc. **517**, 4620 (2022), arXiv:2205.10869 [astro-ph.CO].

[71] F. Beutler, C. Blake, M. Colless, D. H. Jones, L. Staveley-Smith, L. Campbell, Q. Parker, W. Saunders, and F. Watson, The 6dF Galaxy Survey: Baryon Acoustic Oscillations and the Local Hubble Constant, Mon. Not. Roy. Astron. Soc. **416**, 3017 (2011), arXiv:1106.3366 [astro-ph.CO].

[72] A. J. Ross, L. Samushia, C. Howlett, W. J. Percival, A. Burden, and M. Manera, The clustering of the SDSS DR7 main Galaxy sample – I. A 4 per cent distance measure at $z = 0.15$, Mon. Not. Roy. Astron. Soc. **449**, 835 (2015), arXiv:1409.3242 [astro-ph.CO].

[73] S. Alam *et al.* (BOSS), The clustering of galaxies in the completed SDSS-III Baryon Oscillation Spectroscopic Survey: cosmological analysis of the DR12 galaxy sample, Mon. Not. Roy. Astron. Soc. **470**, 2617 (2017), arXiv:1607.03155 [astro-ph.CO].

[74] S. Alam *et al.* (eBOSS), Completed SDSS-IV extended Baryon Oscillation Spectroscopic Survey: Cosmological implications from two decades of spectroscopic surveys at the Apache Point Observatory, Phys. Rev. D **103**, 083533 (2021), arXiv:2007.08991 [astro-ph.CO].

[75] A. G. Adame *et al.* (DESI), DESI 2024 VI: Cosmological Constraints from the Measurements of Baryon Acoustic Oscillations, (2024), arXiv:2404.03002 [astro-ph.CO].

[76] D. Brout *et al.*, The Pantheon+ Analysis: Cosmological Constraints, Astrophys. J. **938**, 110 (2022), arXiv:2202.04077 [astro-ph.CO].

[77] W. Hu and M. J. White, Acoustic signatures in the cosmic microwave background, Astrophys. J. **471**, 30 (1996), arXiv:astro-ph/9602019.

[78] W. Hu and M. J. White, The Damping tail of CMB anisotropies, Astrophys. J. **479**, 568 (1997), arXiv:astro-ph/9609079.

[79] W. Hu, N. Sugiyama, and J. Silk, The Physics of microwave background anisotropies, Nature **386**, 37 (1997), arXiv:astro-ph/9604166.

[80] R. K. Sachs and A. M. Wolfe, Perturbations of a cosmological model and angular variations of the microwave background, Astrophys. J. **147**, 73 (1967).

[81] S. Vagnozzi, Consistency tests of ΛCDM from the early integrated Sachs-Wolfe effect: Implications for early-time new physics and the Hubble tension, Phys. Rev. D **104**, 063524 (2021), arXiv:2105.10425 [astro-ph.CO].

[82] F. Niedermann and M. S. Sloth, Resolving the Hubble tension with new early dark energy, Phys. Rev. D **102**, 063527 (2020), arXiv:2006.06686 [astro-ph.CO].

[83] J. C. Hill *et al.*, Atacama Cosmology Telescope: Constraints on prerecombination early dark energy, Phys. Rev. D **105**, 123536 (2022), arXiv:2109.04451 [astro-ph.CO].

[84] A. La Posta, T. Louis, X. Garrido, and J. C. Hill, Constraints on prerecombination early dark energy from SPT-3G public data, Phys. Rev. D **105**, 083519 (2022), arXiv:2112.10754 [astro-ph.CO].

[85] T. L. Smith, M. Lucca, V. Poulin, G. F. Abellan, L. Balkenhol, K. Benabed, S. Galli, and R. Murgia, Hints of early dark energy in Planck, SPT, and ACT data: New physics or systematics?, Phys. Rev. D **106**, 043526 (2022), arXiv:2202.09379 [astro-ph.CO].

[86] Z.-Y. Peng and Y.-S. Piao, Testing the ns-H0 scaling relation with Planck-independent CMB data, Phys. Rev. D **109**, 023519 (2024), arXiv:2308.01012 [astro-ph.CO].

[87] R. Murgia, G. F. Abellán, and V. Poulin, Early dark energy resolution to the Hubble tension in light of weak lensing surveys and lensing anomalies, Phys. Rev. D **103**, 063502 (2021), arXiv:2009.10733 [astro-ph.CO].

[88] J.-Q. Jiang, G. Ye, and Y.-S. Piao, Impact of the Hubble tension on the $r - ns$ contour, Phys. Lett. B **851**, 138588 (2024), arXiv:2303.12345 [astro-ph.CO].

[89] G. Efstathiou, E. Rosenberg, and V. Poulin, Improved Planck Constraints on Axionlike Early Dark Energy as a Resolution of the Hubble Tension, Phys. Rev. Lett. **132**, 221002 (2024), arXiv:2311.00524 [astro-ph.CO].

[90] L. Pogosian, G.-B. Zhao, and K. Jedamzik, Recombination-independent determination of the sound horizon and the Hubble constant from BAO, Astrophys. J. Lett. **904**, L17 (2020), arXiv:2009.08455 [astro-ph.CO].

[91] K. Jedamzik, L. Pogosian, and G.-B. Zhao, Why reducing the cosmic sound horizon alone can not fully resolve the Hubble tension, Commun. in Phys. **4**, 123 (2021), arXiv:2010.04158 [astro-ph.CO].

[92] V. Poulin, T. L. Smith, R. Calderón, and T. Simon, On the implications of the 'cosmic calibration tension' beyond H_0 and the synergy between early- and late-time new physics, (2024), arXiv:2407.18292 [astro-ph.CO].

[93] D. Pedrotti, J.-Q. Jiang, L. A. Escamilla, S. S. da Costa, and S. Vagnozzi, Multidimensionality of the Hubble tension: the roles of Ω_m and ω_c, (2024), arXiv:2408.04530 [astro-ph.CO].

[94] G. Ye, B. Hu, and Y.-S. Piao, Implication of the Hubble tension for the primordial Universe in light of recent cosmological data, Phys. Rev. D **104**, 063510 (2021), arXiv:2103.09729 [astro-ph.CO].

[95] J. S. Cruz, F. Niedermann, and M. S. Sloth, A grounded perspective on new early dark energy using ACT, SPT, and BICEP/Keck, JCAP **02**, 041, arXiv:2209.02708 [astro-ph.CO].

[96] J.-Q. Jiang, G. Ye, and Y.-S. Piao, Return of Harrison–Zeldovich spectrum in light of recent cosmological tensions, Mon. Not. Roy. Astron. Soc. **527**, L54 (2023), arXiv:2210.06125 [astro-

ph.CO].

[97] H. Wang, G. Ye, J.-Q. Jiang, and Y.-S. Piao, Towards primordial gravitational waves and $n_s = 1$ in light of BICEP/Keck, DESI BAO and Hubble tension, (2024), arXiv:2409.17879 [astro-ph.CO].

[98] H. Wang and Y.-S. Piao, Dark energy in light of recent DESI BAO and Hubble tension, (2024), arXiv:2404.18579 [astro-ph.CO].

[99] R. Kallosh and A. Linde, Hybrid cosmological attractors, Phys. Rev. D **106**, 023522 (2022), arXiv:2204.02425 [hep-th].

[100] G. Ye, J.-Q. Jiang, and Y.-S. Piao, Toward inflation with ns=1 in light of the Hubble tension and implications for primordial gravitational waves, Phys. Rev. D **106**, 103528 (2022), arXiv:2205.02478 [astro-ph.CO].

[101] E. Fondi, A. Melchiorri, and L. Pagano, No evidence for EDE from Planck data in extended scenarios, JHEAp **39**, 14 (2023), arXiv:2203.12930 [astro-ph.CO].

[102] M. Tristram *et al.*, Cosmological parameters derived from the final Planck data release (PR4), Astron. Astrophys. **682**, A37 (2024), arXiv:2309.10034 [astro-ph.CO].

[103] M. Rashkovetskyi, J. B. Muñoz, D. J. Eisenstein, and C. Dvorkin, Small-scale clumping at recombination and the Hubble tension, Phys. Rev. D **104**, 103517 (2021), arXiv:2108.02747 [astro-ph.CO].

[104] J. U. Lange, nautilus: boosting Bayesian importance nested sampling with deep learning, Mon. Not. Roy. Astron. Soc. **525**, 3181 (2023), arXiv:2306.16923 [astro-ph.IM].

[105] K. N. Abazajian *et al.* (CMB-S4), CMB-S4 Science Book, First Edition, (2016), arXiv:1610.02743 [astro-ph.CO].

[106] P. Ade *et al.* (Simons Observatory), The Simons Observatory: Science goals and forecasts, JCAP **02**, 056, arXiv:1808.07445 [astro-ph.CO].